

# Development and research of layered composite materials based on $\text{Cu}_2\text{ZnSnS}(\text{Se})_4$ for solar cells

*A. V. Umarov*<sup>1,2\*</sup>, *B. A. Mirsalixov*<sup>1</sup>, *D. K. Djumabayev*<sup>1</sup>, *F. X. Xusnuddinov*<sup>1</sup>

<sup>1</sup>Tashkent State Transport University, Tashkent, Uzbekistan

<sup>2</sup>Tashkent University of Applied Sciences, Tashkent, Uzbekistan

**Abstract.** This paper discusses the development of manufacturing technology with low costs for the production of solar cells based on  $\text{Cu}_2\text{ZnSnS}(\text{Se})_4$  crystals, elucidation of the physical principles of operation and the search for solutions to improve the efficiency of converting solar energy into electrical energy. The morphology of grown ingots and some electrophysical properties of  $\text{Cu}_2\text{ZnSnS}(\text{Se})_4$  crystals were studied.

## 1 Introduction

To meet the energy needs of the population of remote areas of the republic, it is advisable to use, along with traditional types of energy, environmentally friendly, non-traditional and renewable energy sources (RES). In remote regions where the centralized power system is unreliable or non-existent, the use of RES is the only solution to the problem. Therefore, recently much attention has been paid to the use of renewable energy sources, the production of energy from which is not associated with the consumption of various types of energy carriers.

Composite layered materials based on compounds  $\text{Cu}_2\text{ZnSnS}_4$  (CZTS),  $\text{Cu}_2\text{ZnSnSe}_4$  (CZTSe), and their solid solutions - CZTSSe are promising materials for the manufacture of solar photoconverters [1 – 4]. In terms of optical properties, they favorably differ from other compounds of this class. However, the study of the regularities of the formation of crystals and films, the study of their electrical and optical properties, depending on the technological mode of production, have not been studied.

The purpose of this study is to study the process of obtaining composite materials based on CZTSSe layered films obtained by various methods and to study the electrical properties of the compositions.

## 2 Methods

In order to test the applicability of the devices and test the joints with various materials, the surfaces of the resulting layers were analyzed in detail. Surface analysis revealed a uniform thickness distribution. The atomic force microscopy (AFM) micrographs indicated the

---

\*Corresponding author: [iscmmstiai2022@gmail.com](mailto:iscmmstiai2022@gmail.com)

presence of smooth surfaces, the crystalline nature of the deposited films, and the size of crystallites less than 300  $\mu\text{m}$ , which contributes to the broadening of the peaks in the X-ray diffraction patterns. The AFM method was used for a more detailed analysis of the surface topography. From the three-dimensional representations obtained for the  $\text{Cu}_2\text{ZnSnS}(\text{Se})_4$  layers, it was possible to find a uniform distribution of crystalline domains. The sectional analysis of layers at different points also demonstrated regular topography. At the same time, it is shown that the grain size of crystallites is in the range of 240 – 330  $\mu\text{m}$ .

In this article, we study the creation of anisotype  $\text{Cu}_2\text{ZnSnS}_4/\text{Si}$  HPCMs on a polycrystalline Si matrix.

Samples for research were made by two methods. Vacuum deposition method and centrifugal coating method.

According to the first method the formation of a thin CZTS composite layer on a Si matrix was carried out in two stages. At the first stage, base layers of composite components were formed on a matrix of polycrystalline Si by vacuum deposition. The process was carried out on the installation VUP-5M, under vacuum  $(2-5)10^{-5}$  mm Hg. The ratio of the components of the compositions in the base layer was taken in accordance with the stoichiometric composition of the compound. The latter was calculated based on the atomic weight of the components and the layer thickness of each component of the composition.

At the second stage, the base layer was sulphurized from an unlimited source, in a closed volume. To do this, samples of polycrystalline Si with components of the compositions deposited on the surface were placed in an evacuated to  $(1-3)10^{-5}$  mm Hg. vacuum quartz ampoule. To ensure uniform sulphurization and prevent the evaporation of sulfur from the formed film, sulfur was placed in the ampoule in an amount that provided the required pressure inside the ampoule. The process of formation of the CZTS composite layer was carried out by thermal annealing of samples with base layers in a SUOL-4 furnace. To study the formation of CZTS layers on Si, the components of the compositions were deposited sequentially or in parallel; during sequential deposition, the sequence of deposition of the composition components was varied. The film thickness after each stage of deposition was controlled by the metallographic method. Thermal firing of the components of the compositions was carried out at temperatures of 400 - 620<sup>0</sup> C, the firing time was in the range of 15 - 90 minutes. The heating rate was 15 - 30 degrees/min. After firing, the samples were cooled to 200<sup>0</sup> C at a rate of 10 - 15 deg./min., and then brought to room temperature by pulling the ampoules out of the oven or together with the oven.

An alternative method for the deposition of thin semiconductor layers, which avoids some of the above disadvantages, is the method of deposition from solutions. At present, various applications of this method for processing both inorganic [5 - 9] and organic [10 - 16] semiconductors are known and registered. This method offers the possibility of processing semiconductor layers in ambient conditions at no cost due to the need to create a vacuum. At the same time, this method provides more opportunities to control the growth dynamics, composition and morphology of thin layers due to effective work with: concentrations of the solutions used, substrate speeds in the case of semiconductor layer deposition by centrifugation, change in dopant concentration in situ, change in ambient temperature and etc. The possibility of changing the concentration of the dopant in situ facilitates further studies of its contribution to the concentration of voids, which, in turn, has an obvious contribution to the photocurrent generated by the fabricated photovoltaic devices. Another very important advantage of this method is the possibility of obtaining bulk heterojunctions by treating materials with donor and acceptor electronic properties in the same solvent or in specific mixtures of compatible solvents. Finally, according to recent studies [17], this method allows to obtain printed solutions from semiconductor materials,

which opens up the possibility of mass production of photovoltaic devices with low cost and full efficiency that meets modern requirements.

The main processes for depositing thin layers in solutions are spinning, drip casting, dripping, printing, dip coating and Langmuir-Blodgett, as well as spray pyrolysis. Considering the fact that the last two of the above processes result in too thin  $\text{Cu}_2\text{ZnSnS}_4$  layers for the development of photovoltaic devices, as well as the lack of equipment for printing solutions in our research laboratory, special attention was paid to deposition methods. centrifugation and dripping, which allows better control of the thickness of thin layers.

Evaporation is a complex process in which part of the excess solvent is absorbed by the atmosphere and plays an important role in thinning the film formed during centrifugation (Figure 1). To obtain quality films without defects, a careful analysis of the correlation between the solvent evaporation rate and the rate is necessary. The film thickness is approximately inversely proportional to the square root of the rotation speed.

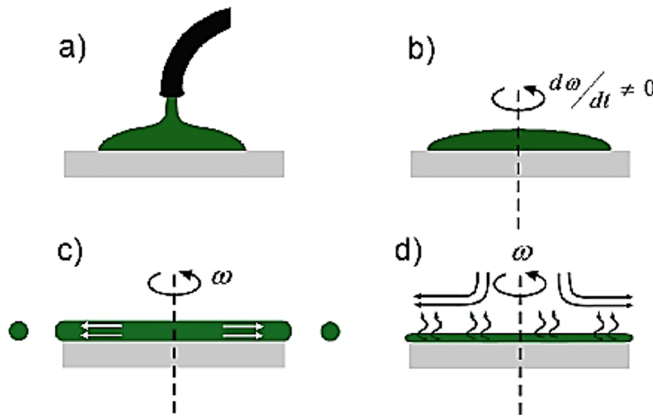


**Fig. 1.** Stages of deposition of the thin layer by centrifugation [18]

The drying rate of the film during the wringing process depends on the nature of the liquid itself (the volatility of the solvent systems used) as well as on the temperature and humidity of the air surrounding the substrate during the wringing process. It is also very important that the airflow and associated turbulence over the substrate be kept to a minimum, or at least brought to a constant speed, during the wringing process.

The differential equation that describes the variation in time of the height of the layer deposited by centrifugation has the form:

$$\frac{\partial h}{\partial t} = -2Kh^3 - E \quad (1)$$

where  $E$  is the evaporation rate of the solvent, and  $K$  is the coefficient corresponding to the centrifugation step, which depends on the speed and viscosity of the liquid.

Before explicitly solving this equation, Meyerhofer assumed that at the initial stages of the flattening process, the solution flow displaced from the substrate completely dominates, and at the final stages, the evaporation rate almost completely dominates. [19] He set the transition point under the condition that the rate of evaporation and the rate of flow become equal. It could be fifty considered to be the hydrodynamic point in the spin coating process, after which the evaporation now depends on the speed of the substrate,  $\omega$ . In this way

$$E = C\sqrt{\varepsilon} \quad (2)$$

where the proportionality constant C must be determined from specific experimental conditions. It should be noted that such a radical dependence is observed for laminar air flow over a rotating substrate. [20]

Karpichka et al. also solved equation (1.1) analytically for a constant solvent evaporation rate. According to them, the amount of material deposited per unit area at the end of the dry film forming process is [21]:

$$G = \frac{N(h \rightarrow 0)}{A} \approx 0.8c_0 \left(\frac{E}{K}\right)^{\frac{1}{3}} \approx \left(\frac{E}{3v}\right)^{\frac{1}{3}} \omega^{-\frac{1}{2}} \quad (3)$$

Here N is the amount of material and A is the surface area of the substrate. Equation (1.2) shows that the amount of deposited material can be controlled by knowing the initial concentration ( $c_0$ ) of the solution, the rate of evaporation of the solvent (E) and the rate ( $\omega$ ).

Advantages of centrifugal coating method:

1) The thickness of the thin layer can be easily changed by changing the rotation speed and the concentration of the solution.

2) Thin layers with high thickness uniformity can be obtained.

3) The distribution of the material in the deposited thin layer is uniform.

4) The resulting thin layers have very good adhesion to the substrate.

Disadvantages of the method:

1) Large substrates cannot always be centrifuged at a high enough speed.

2) A large amount of solution is ejected from the substrate.

3) Obtaining a thin semiconductor layer requires relatively long time intervals (3-4 hours depending on the type of applied material and the required thickness).

Manufacturing technology of photovoltaic devices based on processed layers.

For the production of prototypes of photovoltaic devices based on processed thin layers from chemical solutions, Si substrates were used, which for cleaning pre-sonicated in acetone or isopropyl alcohol, then washed with distilled water and dried in a stream of hydrogen or directly in the centrifuge boat. Subsequently, over the substrates buffer layer was applied by centrifugation at 1500 revolutions / min with thickness 120 nm. Then, solutions were applied over this layer both by the drop method and by centrifugation.

After drying thin layers at room temperature, some of them were

thermally processed. Aluminum electrodes were deposited by the method high vacuum thermal evaporation from molybdenum and/or tungsten boats. For evaluation purposes measurements of photovoltaic parameters were carried out both immediately after the manufacture of devices and

extracting them from a high vacuum, as well as after keeping them in the air in a room for certain periods of time (2h -72h  $\rightarrow$  6 months).

Experimental studies were carried out on solar cells of the Schottky diode type, compositions based on  $\text{Cu}_2\text{ZnSnS}_4/\text{Si}$  obtained by the above two methods with a thickness (2.1  $\mu\text{m}$ -8  $\mu\text{m}$ ) of active layers Zinc phthalocyanine is processed from solutions with a concentration of 98% LC as a solvent.

### 3 Results and Discussion

Studied the current-voltage characteristics of layered structures  $\text{Cu}_2\text{ZnSnS}_4/\text{Si}$  Schottky diode obtained by 1- vacuum deposition method and 2- centrifugation method.

Figure 2 illustrates the J-U characteristic of layered structures  $\text{Cu}_2\text{ZnSnS}_4/\text{Si}$  Schottky diode obtained by 1- vacuum deposition method and 2- centrifugation method. These studies clearly demonstrate the behavior of straightening in the dark, which is enhanced during the preparation of the composition by vacuum deposition. The active surface of the composition is about  $1.5 \text{ cm}^2$ , and the layer thickness is almost  $5 \mu\text{m}$ . By applying a negative voltage to the aluminum electrode, the current strength was measured at various voltage values in the range from 0 to 10 V at room temperature. From the current-voltage characteristics for direct polarization of layered compositions, both obtained by vacuum deposition and centrifugation, we observe an asymmetric behavior and an improvement in electrical conductivity obtained by vacuum deposition

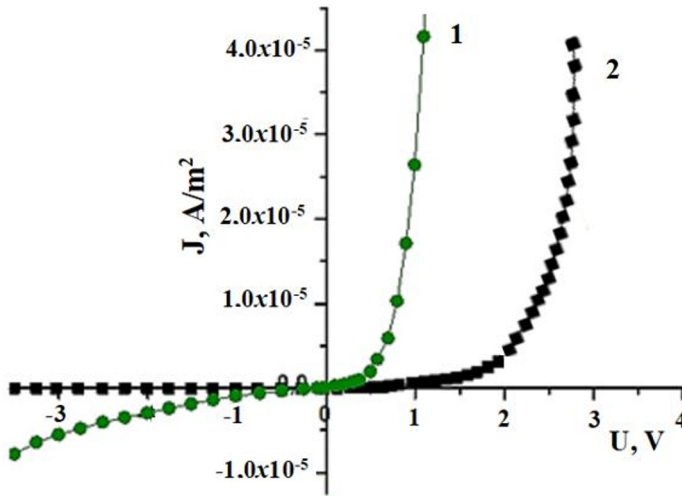


**Fig. 2.** Current-voltage characteristics of layered structures  $\text{Cu}_2\text{ZnSnS}_4/\text{Si}$  Schottky diode obtained by 1- vacuum deposition method and 2- centrifugation method.

It is observed that at low values of the direct voltage, the current varies with the voltage according to a linear legitimacy, and at high values of the voltage the dependence of the voltage current density is exponential. The dynamic resistance  $R_d$  is determined experimentally from the linear slope of the current-voltage characteristic, according to the relation:

$$R_d = \Delta U / \Delta J \quad (4)$$

As a result of obtaining the composition by vacuum deposition, the surface resistance of the composition decreased from  $R_d = 3.8 \cdot 10^4 \Omega \cdot \text{m}^2$  to  $9 \cdot 10^3 \Omega \cdot \text{m}^2$ . In order to determine the mechanism of current transport through the structures under study, the direct branches of the J-U characteristic were reconstructed.

on a logarithmic scale (Fig. 3). Two linear slopes are observed, which confirm the different mechanisms of transport of electric charge carriers when applying different values of DC voltage. The exponential dependence in the region of higher voltages can be explained by the formation of a space charge region between the layers of the composition. Note that

when voltages are applied above 0.6 and 1.0 V at room temperature, the Schottky barrier effect disappears.

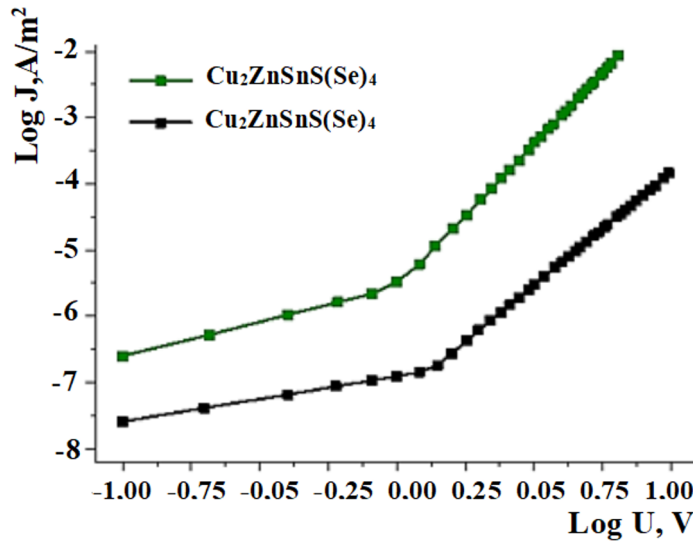


**Fig. 3.** Current-voltage characteristics of the direct branch on a logarithmic scale a layered compositions obtained by 1- vacuum deposition method and 2- centrifugation method.

At direct polarization, the slope of the characteristics in the voltage range up to almost 1 V indicates the value of  $m$  of the order of the unit, which describes an ohmic conduction mechanism. The current density in the ohmic conduction region is described by the equation:

$$J = p_0 e \mu \frac{U}{d} \quad (5)$$

where the concentration of thermally generated voids ( $p_0$ ) is determined according to equation [22]:

$$p_0 = N_v \exp \left[ \frac{-(E_F - E_v)}{kT} \right] \quad (6)$$

where  $(E_F - E_v)$  is the separation of the Fermi level from the edge of the valence band, and  $N_v$  the density of the states in the valence band. Substituting (4.3) into (4.2) results in the density of the electric current:

$$J = N_v e \mu \left( \frac{U}{d} \right) \left[ \frac{-(E_F - E_v)}{kT} \right] \quad (7)$$

**Table 1.** Electrical parameters  $E_F$ ,  $\mu$  and  $p_0$  of the layered compositions obtained by 1- vacuum deposition method and 2- centrifugation method

Parameters	obtained by 1- vacuum deposition method	obtained by 2 - centrifugation method
$E_F$ (eV)	0.51	0.57
$\mu$ ( $\text{cm}^2/\text{V}\cdot\text{s}$ )	$1.1\cdot 10^{-2}$	$1.2\cdot 10^{-2}$
$p_0$ ( $\text{cm}^{-3}$ )	$5.0\cdot 10^{11}$	$6.3\cdot 10^{12}$

From Table 1 it can be seen that in the samples obtained by the 1-method,  $p_0$  increases by one order of magnitude, and  $\mu$  by approximately two orders of magnitude, which can be explained by the fact that at an electron acceptor, and on the other hand, promotes the interaction of the molecules of the composition in the treated layers, facilitating the transfer of charges through them. With direct polarization (Fig. 2), when voltages above 1 V are applied, a quadratic dependence of the voltage current density is observed, which is described by a power law as

$$J \sim U^m \quad (8)$$

Calculating the value of the index  $m$  (index  $m$  has values  $\geq 2$ ) we can see that the conduction mechanism is the current limited by the space load. The numerical value of this index indicates the presence of traps in the range of the prohibited band, depending on the temperature of the sample and the biased direction. The current density in this region is described by the relation [23, 24]:

$$J = \frac{9}{8} \varepsilon \mu \theta \frac{U^2}{d^3} \quad (9)$$

Where  $\varepsilon$  and  $\mu$  are the electrical permittivity and mobility of zinc phthalocyanine electric charge carriers, and  $\theta$  is the ratio of free and trapped loads and is described by the expression:

$$\theta = \frac{N_v}{N_{t(s)}} \exp\left(-\frac{E_t}{kT}\right) \quad (10)$$

where  $N_t$  is the concentration of traps whose energy level is located in the forbidden band at an energy distance  $E_t$  from the lower edge of the valence band. Then the current density will look like:

$$J = \left(\frac{9}{8}\right) \varepsilon \mu \frac{N_v}{N_{t(s)}} \frac{U^2}{d^3} \exp\left(-\frac{E_t}{kT}\right) \quad (11)$$

the investigated features of the I-U characteristic denote an exponential distribution of the capture states in the passband. We assume that there is an exponential distribution of the capture states in the bandgap, described by a function such as:

$$\rho(E) = \frac{N_t}{kT_C} \exp\left(-\frac{E}{kT_C}\right) \quad (12)$$

where:  $\rho(E)$  is the density of the traps per unit of energy and per unit of volume as a function of the distance  $E$  from the edge of the conduit or valence band;  $T_C$  is the so-called “characteristic temperature”, which is a specific parameter of the trap distribution, which describes the rate of decrease of  $\rho(E)$  with the decrease of energy in  $\rho(E)$  with the increase of energy (for example, at  $T_C \rightarrow \infty$  we obtain a Uniform distribution of blocking states)  $N_t/kT_C$  is the density of blocking states near the edge of the permitted area or at the edge of the blocking state. estimating the ratio  $\Theta$ , which is the fraction of the total number of injected carriers that remain free, and introducing the actual drift mobility  $\mu = \mu_0 \Theta$  in relation to Mott and Gurney [25], which requires the following assumptions:

- only a very small fraction of the injected load remains free to participate in driving, the rest being captured by the capture states,
- the level of Fermi  $E_F$  represents the level of demarcation between the deep traps considered populated with load carriers and the superficial ones considered free,  $-T_C > T$ .

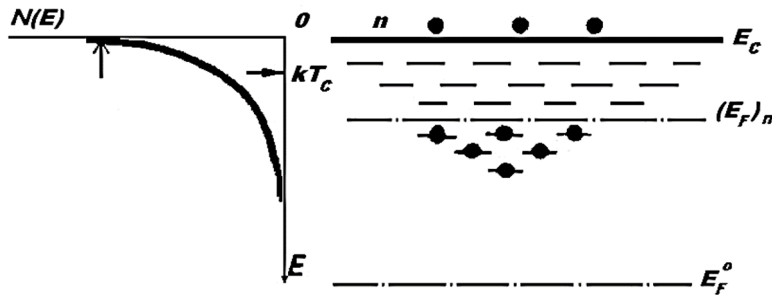


**Fig. 4.** Energy range diagram for compositions with an exponential distribution of capture states

## 4 Conclusions

1. It was shown that layered compositions based on  $\text{Cu}_2\text{ZnSnS}_4/\text{Si}$  form Schottky barriers with ohmic contacts of Al and molybdenum. The rectification factor increases when obtained by vacuum deposition.

2. Layered compositions based on  $\text{Cu}_2\text{ZnSnS}_4/\text{Si}$  obtained by vacuum deposition resistance  $r_d = 3.8 \cdot 10^4 \Omega \cdot \text{m}^2$ , and by centrifugation it reaches  $9 \cdot 10^3 \Omega \cdot \text{m}^2$ .

3. For the resulting composite samples based on  $\text{Cu}_2\text{ZnSnS}_4/\text{Si}$  obtained by both methods, at voltages up to almost 1 V, the ohmic conduction mechanism prevails ( $m \sim 1$ ), and at voltages above 1 V, the driving mechanism is the current limited by the space charge ( $J \sim U^m$ ).

4. The study of the current–voltage dependence showed that, on the logarithmic scale  $\text{JU}$ , the characteristics of compositions at relatively high voltages are nonlinear and also obey a power law with a power factor  $m > 2$  at 295 K.

5. The coefficient  $m$  increases with decreasing temperature.

6. The model of a spatial current limited by one volume load was used to interpret the experimental data of the  $\text{Cu}_2\text{ZnSnS}_4/\text{Si}$  compositions.

7. According to the characteristic  $\text{I}f(U)$  at various measurement temperatures (90 ... 295) K, it was found that in the region of low voltages below the value of the transient



voltage  $U < 2.4 V$ , the ohmic conduction mechanism prevails, and at higher applied voltages at the transient voltage  $U > 2.4 V$ , the mechanism of conducting load currents of a limited volume with an exponential distribution of capture states prevails.

## References

1. Susanne Siebentritt<sup>1</sup> and Susan Schorr. *Prog. Photovolt: Res. Appl.* 2012; 20:512–519.
2. Li J., Ma T., Liu W. et al. // *Appl. Surf. Sci.* 2010. V.258. Iss. 17. p. 6261–6265.
3. Arun Khalkar, Kwang-Soo Lim, Seong-Man Yu, Shashikant P. Patole, and Ji-Beom Yoo. *International Journal of Photoenergy.* 2013, V. 201, Article ID 690165, 7pages.
4. Magrupov, M.A., Umarov, A.V., Khamidov, Sh.R., Makhmudov, R.Kh.
5. *Elektrichestvo*, 1994, (6), p. 70–72.
6. T.K. Townsend, D. Durastanti, W.B. Heuer, E.E. Foos, W. Yoon, J.G. Tischler, Fabrication of Fully Solution Processed Inorganic Nanocrystal Photovoltaic Devices, *Journal of Visualized Experiments.* 113 (2016) 1-9.
7. Li. Liang, N. Coates, D. Moses, Solution-Processed Inorganic Solar Cell Based on In Situ Synthesis and Film Deposition of CuIn<sub>2</sub>S<sub>3</sub> Nanocrystals, *Journal of The American Chemical Society.* 1 (2010) 22-23.
8. Z. Qiu, C. Liu, G. Pan, W. Meng, W. Yue, J. Chen, M. Wang, Solution-Processed Solar Cells Based on Inorganic Bulk Heterojunctions with Evident Hole Contribution to Photocurrent Generation, *Physical Chemistry Chemical Physics.* 17 (2015) 12328–12339.
9. T.K. Townsend, E.E. Foos, Fully Solution Processed All Inorganic Nanocrystal Solar Cells. In: *Physical Chemistry Chemical Physics.* 16 (2014) 16458–16464.
10. Magrupov, M.A., Umarov, A.V., Khamidov, Sh.R., Makhmudov, R.Kh.
11. *Glass and Ceramicsthis*, 1992, 49(7), p. 313–314
12. C.J. Brabec, J.R. Durrant, Solution-Processed Organic Solar Cells. In: *MRS Bulletin.* 33 (2008) 670–675.
13. Z. Tang, A. Elfving, A. Melianas, J. Bergqvist, Q. Bao, O. Inganäs, Fully-Solution-Processed Organic Solar Cells with A Highly Efficient Paper-Based Light Trapping Element, *Journal of Materials Chemistry A.* 3 (2015) 24289–24296.
14. Y. Yang, G. Li, Progress in High-Efficient Solution Process Organic Photovoltaic Devices. *Topics in Applied Physics.* Springer, (2015).
15. J.T. Bloking, X. Han, A.T. Higgs, J.P. Kastrop, L. Pandey, J.E. Norton, A. Sellinger, Solution-Processed Organic Solar Cells with Power Conversion Efficiencies Of 2.5% Using Benzothiadiazole/Imide-Based Acceptors, *Chemistry of Materials.* 23 (2011) 5484–5490.
16. C. Cui, Y. Zhang, W. Choy, H. Li, W.-Y. Wong, Metallated Conjugation in Small-Sized-Molecular Donors for Solution-Processed Organic Solar Cells, *Science China Chemistry.* 58 (2015) 347–356.
17. Juraev Sh.T., Ibadullaev A., Muhiddinov B.F., Xusenov K.Sh., *International Journal of Advanced Science and Technology* Vol. 29, No. 9s, (2020), pp. 4111-4118 ISSN: 2005-4238 IJAST.
18. Margrupov, M.A., Umarov, A.V., Saidkhodzhaeva, K.Sh., Kasimov, G.A.
19. *Plasticheskie Massy: Sintez Svoystva Pererabotka Primenenie*, 1995, (2), p. 26–27

20. S.-H. Bae, H. Zhao Et Al. Printable Solar Cells from Advanced Solution-Processible Materials, *Chem. I* (2016) 171-328.
21. S. L. Hellstrom, *Basic Models of Spin Coating*: Stanford University, 2007. <http://large.stanford.edu/courses/2007/ph210/hellstrom1/>.
22. M.D. Tyona, A Theoretical Study on Spin Coating Technique, *Advances in Materials Research*. 4 (2013) 195-208.
23. D. Meyerhofer. Characteristics of Resist Films Produced by Spinning, *Journal of Applied Physics*. 49 (1978) 3993.
24. S. Karpitschka, C.M., Weber, H. Riegler., *Physics of Spin Casting Dilute Solutions*. Arxiv E-Prints, (2012).
25. R.A. Montani, J.C. Bazán, Electronic Conductivity and Chemical Diffusion Coefficient of Cadmium-Doped Cuprous Iodide, *Solid State Ion*. 46 (1991) 211-216.
26. M. Braik, Et Al. Investigation of Structural, Optical and Electrical Properties of a New Cobalt Phthalocyanine Thin Films with Potential Applications, *Perchlorate Sensor Synthetic Metals*. 209 (2015) 135–142.
27. Mutabar, M.H. Shah Sayyad Kh.S. Karimov. Electrical Characterization of The Organic Semiconductor Ag/Cupc/Au Schottky Diode, *Journal of Semiconductors*. 32 (2011) 044001.
28. Chandra, *Et Al*. Two-Dimensional Analytical Mott-Gurney Law for A Trap-Filled Solid, *Appl. Phys. Lett*. 90 (2007) 153505